Induced Chain Alignment of Conjugated Polymers Within Nanoporous Template

Kuan-Hsin Lo, Rong-Ming Ho, Yung-Ming Liao, Chain-Shu Hsu,* Florian Massuyeau, Yuan-Chun Zhao, Serge Lefrant, and Jean-Luc Duvail**

This work presents a simple method to generate ordered conjugated polymer nanoarrays through a pore-filling process for nanoporous polymer templates so as to enhance the efficiency of photoluminescence (PL). PL results combined with the morphological evolution examined by scanning probe microscopy revealed that the enhanced PL reaches maximum intensity as the template pores are completely filled by conjugated polymers. Polarized PL spectroscopy and grazing incidence Fourier transform infrared spectroscopy were used to determine the chain orientation of templated conjugated polymer; the spectroscopic results indicate a parallel chain orientation along the cylindrical direction of nanopores. The induced alignment of the polymer chains is attributed to a nanoscale spatial effect that increases the PL intensity and the lifetime of the conjugated polymer. The enhanced luminescence of nanostructured conjugated polymers is highly promising for use in designing luminescent nanodevices.

1. Introduction

During the past decade, conjugated polymers have emerged as cost-effective functional materials for organic electronic devices such as solar cells[1,2] and field effect transistors (FETs).[3,4] In organic nanodevices, the size and shape of polymer nanostructures as well as the chain orientation and crystallinity of conjugated polymers have been shown to have strong effects on charge-carrier mobility and overall device performance.[5,6] This is attributed to the anisotropic behavior of charge transport in conjugated polymer, resulting from electrons delocalized along the polymer backbone and the overlap of π-orbitals.[7] In conjugated polymers such as poly(*p*-phenylenevinylene) (PPV), the primary excitations are predominantly associated with the π-orbital structure corresponding to the main spectral features arising from π–π^* transitions.[8,9] As a result, controlling the film architectures with appropriate molecular dispositions is needed to fully exploit the optical and electrical properties of conjugated polymers.[10,11] Moreover, the corresponding polymer morphologies are critical for device performance. For instance, in bulk heterojunction (BHJ) solar cell structures, the control of morphologies in nanoscale plays an important role in exciton dissociation and charge transport.[5] In most cases, the forming morphologies are correlated to chain orientation but it is difficult to control both textures simultaneously and favorably. Several techniques have been reported to promote phase separation in nanoscale to achieve the goals. The Langmuir–Blodgett (LB) technique induces a classical anisotropy in the film between out-of-plane and in-plane properties. As found, rodlike polymers,[12] rodlike polymer crystals,[13] and self-aggregated molecules[14] can be oriented during transfer, resulting in an in-plane anisotropy. Rubbing-induced alignment of segmented PPV precursors has also been used for the preparation of two-layer light-emitting diodes (LEDs) that gave high emission dichroic ratio (DR_E) of linearly polarized electroluminescence.[15]

Non-classical methods for controlling the morphology and chain orientation of conjugated polymers, such as confinement that imposes spatial constraints on polymers, present new opportunities to create specific nanostructures with unique applications. For instance, nanoimprint lithography was used to fabricate large-area, high-density, and ordered nanostructures in conjugated polymers, and also to simultaneously control 3D chain orientation within conjugated polymer nanostructures.[16] Vertical chain alignment was observed in both nanogratings and nanopillars, indicating strong potential to improve charge transport and optical properties for the application as solar cells. When the dimension of a confining volume is less than the radius of gyration, a quantitative realization of disturbances to chain behavior due to spatial constraints remains a challenge.[17–20] With the development of nanofabrication processes, the dynamics of confined polymers have significant applications in nanotechnologies.[21–25] However, understanding the induced chain alignment in defined

Dr. K.-H. Lo, Prof. R.-M. Ho
Department of Chemical Engineering
National Tsing Hua University Hsinchu 30013, Taiwan
E-mail: rmho@mx.nthu.edu.tw
Dr. Y.-M. Liao, Prof. C.-S. Hsu
Department of Applied Chemistry
National Chiao Tung University Hsinchu 30013, Taiwan
E-mail: cshsu@mail.nctu.edu.tw
Dr. F. Massuyeau, Dr. Y.-C. Zhao, Prof. S. Lefrant, Prof. J.-L. Duvail
Institut des Matériaux Jean Rouxel
UMR6502 CNRS
University of Nantes F-44322 Nantes, France
E-mail: duvail@cnrs-imn.fr

DOI: 10.1002/adfm.201002573

Table 1. Characteristics of DP-PPV-PEO copolymers.

code	M_n[a)] [g/mol]	PDI	Solvent
PVE3	10309	1.12	Acetic acid
PVE7	14866	1.10	Acetic acid

[a)]Measured from GPC analysis.

nanostructures, in particular in thin-film systems, remains challenging. The self-assembly of soft matter is one of the most convenient means of creating nanostructures with functions and complexity. Self-assembled morphologies from block copolymers (BCPs) satisfy the size requirement for nanodevices.[26–31] BCP thin-film samples with nanoporous textures could be obtained by chemically removing one constituted block using UV,[32,33] oxygen plasma,[34] and base aqueous solution.[35,36] In our previous studies, a series of polylactide-containig BCPs have been synthesized to construct nanoporous polymeric thin films from the self-assembly of the BCPs after hydrolysis, and then used as templates for pore-filling process.[37–41] In this study, we aim to create nanostructured thin film with cylindrical nanostructures through pore-filling poly(2,3-diphenyl-5-(trimethylene-octa(oxyethylene)-methoxy)-phenylene vinylene) (DP-PPV-PEO) conjugated polymers into the nanoporous templates. To successfully accomplish the pore-filling process, a series of hydrophilic conjugated polymers, DP-PPV-PEO, were synthesized. The polymerization was carried out via a modified Gilch route to obtain hydrophilic DP-PPV-PEO with different lengths of PEO segment. **Table 1** presents the characteristics of represented samples as PVE3 and PVE7. Via a specific pore-filling process, i.e., a solvent-annealing process, the PVE can be successfully introduced into the templates to form a well-defined PVE nanostructure (as shown in Scheme S1). In contrast to a simple PVE thin film, the luminescence intensity of the PVE emission can be significantly enhanced for templated PVE nanoarrays. The variation is attributed to the enhanced chain alignment of PPV backbone, as demonstrated by the results of polarized photoluminescence (PL) spectroscopy combined with grazing incidence Fourier transform infrared (GI-FTIR). The time-resolved PL decay data also revealed longer lifetime for templated PVE nanoarrays. As a result, the enhanced luminescence is mainly attributed to nanoscale spatial effect, ultimately inducing the chain orientation of PPV that significantly alleviates the self-quenching problem.

2. Results and Discussion

Figure S1 (Supporting Information (SI)) shows the transmission electron microscopy (TEM) image of the nanoporous PS template, resulting from the self-assembly of polystyrene-*b*-poly(L-lactide) (PS-PLLA) after hydrolysis of PLLA, at which the PS appears as gray matrix and the nanopores are the bright regions due to mass–thickness contrast. Following solvent annealing, PEV3 and PEV7 can be successfully pore-filled into the nanoporous PS template. As shown in **Figure 1**a and Figure 1b, templated PEV nanoarrays with significant dark

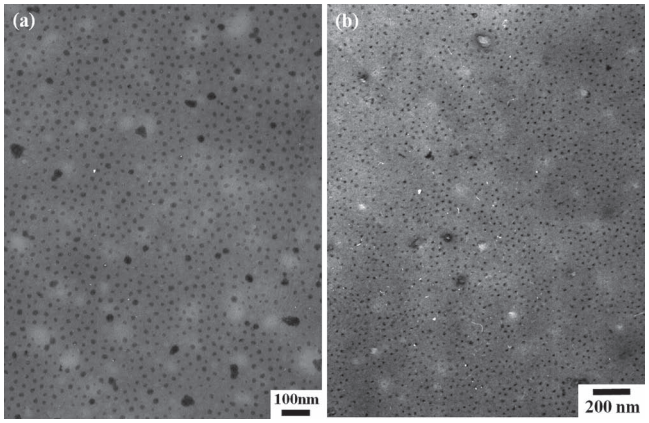

Figure 1. TEM images of templated a) PVE3; b) PVE7 nanoarrays with PTA staining.

contrast dispersed in the gray PS matrix can be clearly identified due to the potassium phosphotungstate (PTA) staining for PEO segment. Steady-state photoluminescence (PL) spectra were acquired to measure the luminescence of nanostructured thin film before and after solvent annealing. Before solvent annealing, the PL spectra of PEV3 and PEV7 thin films are shown in **Figure 2** as solid lines. The polymer films with the broad band blue–green PL emission exhibit similar vibronic features with the maximum emission peaks around 498 nm and the shoulder peaks at 533 nm, suggesting a significant blue shift compared with the emission peaks (520 and 551 nm) of the PPV homopolymer. Such blue shift is attributed to the steric effect resulting from the bulky substituents in PPV.[42] The bulky pendent groups force phenylene rings or vinylene groups to twist around the PPV backbone, resulting in a loss of total co-planarity of the main chain p-system. Such a twist partially disrupts the p-delocalization, which, in turn, is expected to increase bandgap energies and causes the blue shift. By contrast, after solvent annealing, the PL intensity of templated PVE nanoarrays significantly increases (Figure 2a and Figure 2c). For comparison, spin-coated PVE thin film was prepared by the same solvent-annealing process without using the nanoporous PS template. Instead of an increase in PL intensity, the PL spectrum of spin-coated PVE thin film (Figure 2b and Figure 2d) reveals an observable decrease in the emission intensity after solvent annealing because of the occurrence of the self-quenching problem. Accordingly, we speculate that the pore-filling of PVE polymers within the nanoporous PS template generates a nanoscale spatial effect that greatly changes the luminescence behavior due to the induced chain alignment of the PPV chains (see below for discussion). The suggested nanoscale spatial effect is different from the capillary-driven effect on polymer chains. As demonstrated, by taking advantage of a solution wetting process via capillary action, anisotropic chain orientation can be obtained by driving the PAN chains into an anodic aluminum oxide (AAO) membrane template.[43] Since the dimensions of the mesoscopic AAO pores are significantly larger than the size of the PAN chain, the effect of capillary force-driven behavior on the induced chain orientation far outweighs that of confinement effects arising from spatial

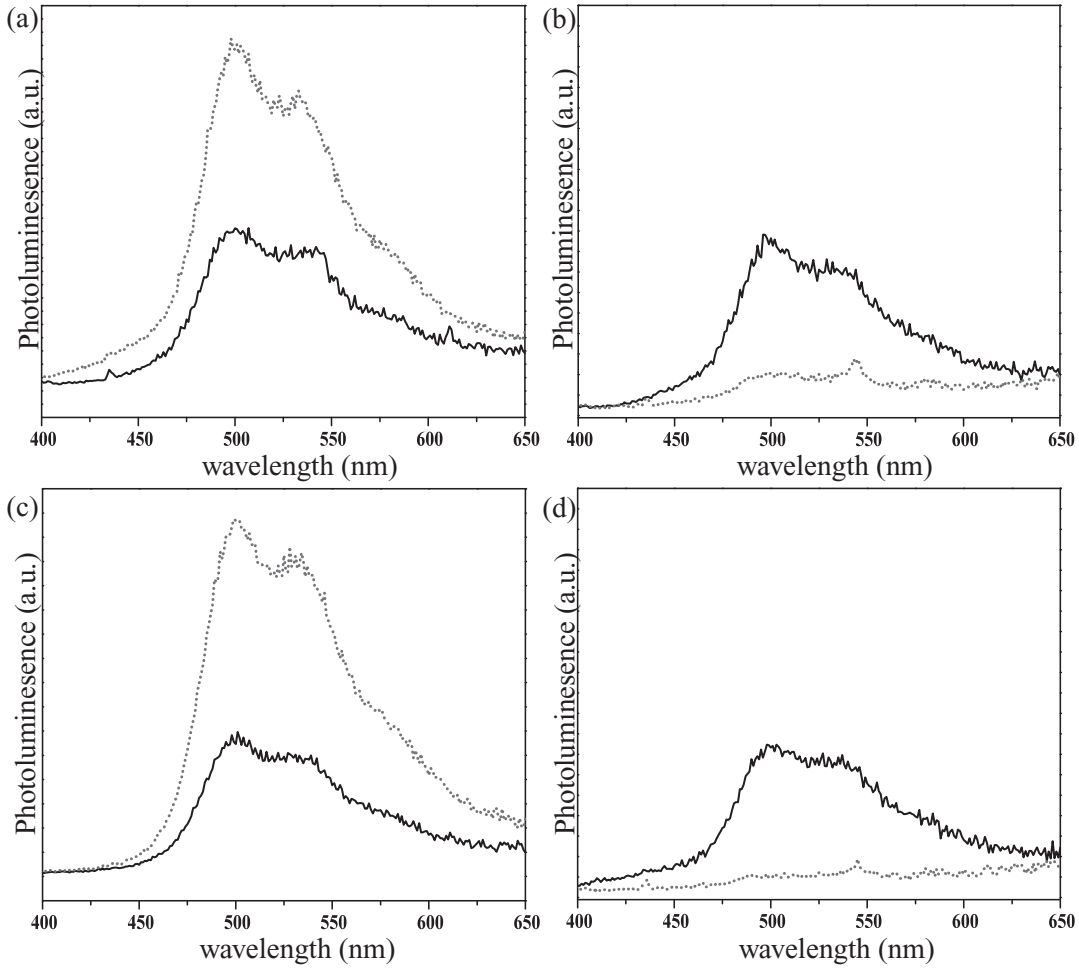

Figure 2. PL spectra of spin-coated PVE3 and PVE7 thin films on glass substrate; a,c) with and b,d) without the deposition of nanoporous PS template before (solid line) and after (dot line) solvent annealing for 48 hr.

constraint. The capillary-force driven anisotropy of chain orientation is intrinsically of kinetic origin because the induced orientation via the solvent-annealing process is dependent upon the control of solvent evaporation rate. In contrast, the induced anisotropy of chain orientation by the nanoscale spatial effect is in principle of a thermodynamic origin. As demonstrated by Shin and co-workers, polymer chains can be compressed in a direction orthogonal to the flow because of the spatial constraint (i.e., the confinement) as the polymers were induced into the nanopores with diameter smaller than the size of polymer chain.[20] The confinement effect would be retained even after long-time annealing whereas the capillary-driven behavior might be released after thermal annealing.

To further examine the suggested nanoscale spatial effect, the nanoporous PS template on spin-coated PVE thin film was treated with solvent annealing for PL measurement at different accumulated annealing times. Corresponding morphological evolution was traced by using scanning probe microscopy (SPM). As shown in the inset of **Figure 3**a and Figure 3b, the PL intensity of PVE peak increases with annealing time and then reaches a maximum at 48 hr. With further annealing, the intensity of PVE peak decreases significantly. Figure 3b and Figure 3d show the morphological evolution of the thin-film sample; the initial morphology reveals the surface of nanoporous PS template with a height difference of 8~11 nm at annealing time t = 0 (see Figure S2, SI). With the increase of annealing time, the PVE can then be introduced into nanopores by capillary force. After solvent annealing treatment for 24 hr, the partially filled template reveals the decrease of height difference to 2~4 nm. With further annealing to 48 hr, the majority of nanopores can be filled with the PVE. The pore-filling process is driven by capillary force, dependent upon the surface tension of wetting substrate (i.e., PS template) and the wetting tendency for the solution onto the substrate (i.e., the interfacial energy of PS and solution).[36,39,40] In this study, the vapor of acetic acid is used to promote the wetting tendency of the PVE onto nanoporous PS template for pore-filling through capillary rise; this approach is referred to solvent-annealing process. Upon exposure to acetic acid vapor, the acetic acid swells the PVE, and then drives the PVE into the nanoporous template due to the increase on PVE chain mobility. After solvent annealing for 72 hr, the PS surface is covered by the PVE due to the strong affinity between PVE chain and acetic acid. The capillary rise of a polymeric liquid in a nanoporous template has been studied by Shin and

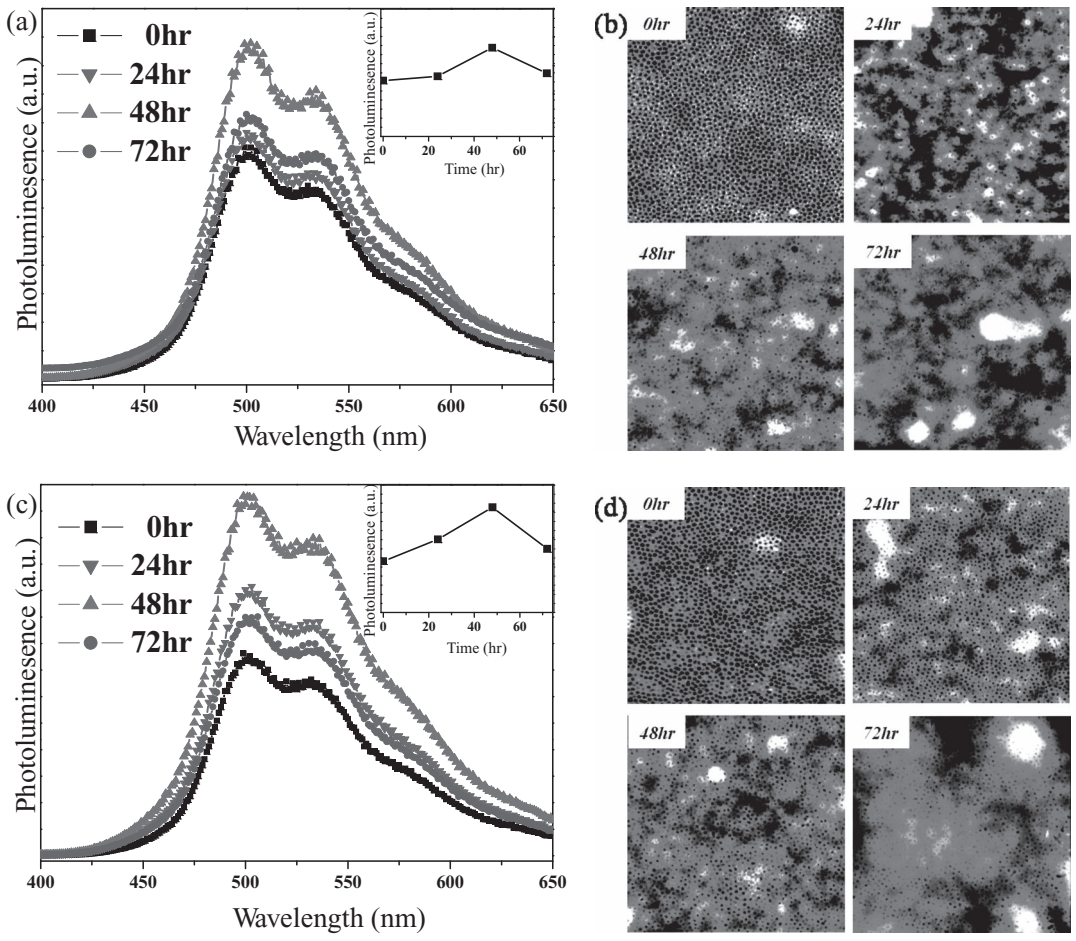

Figure 3. PL spectra of nanoporous PS templates on spin-coated a) PPV3 and c) PPV7 thin films for different solvent-annealing times. Insets show the plots of the intensity of first peak (498 nm) versus annealing time. SPM tapping-mode height images of nanoporous PS templates on spin-coated b) PPV3 and d) PPV7 thin films for different solvent-annealing times. The scale of the SPM image is 2 μm × 2 μm.

co-workers recently; as found, an overflow of polymer melt onto the surface may occur.[20] Similarly, the PVE polymer tends to surface out from the nanopore due to the affinity of acetic acid vapor with PVE polymer; after 72 hr solvent annealing, the formation of PVE wetting layer on the top of the nanoporous PS template can be found because of the merging of surfaced PVE film. **Scheme 1** illustrates the morphological evolution of pore-filling PVE into naoporous PS template. The morphological evolution corresponds well with the observed changes of the PL spectra of pore-filled PVE. Once the PVE releases from the nanopores through pore-filling, in addition to the annihilation of nanoscale spatial effect, the polymer chains in the wetting layer are randomized by further solvent annealing so as to cause a significant self-quenching problem. As suggested, the enhancement in luminescence is mainly attributed to the chain alignment of conjugated polymer induced by spatial constraint.

To investigate the PVE chain alignment induced by the nanoscale spatial effect, polarized PL spectroscopic experiments was conducted to measure the polymer orientation in thin film. With regard to the polarization dependence of PL data, the spectra were acquired under conditions of vertically polarized excitation with vertically (VV) and horizontally (VH) polarized collection, respectively. It is noted that the horizontally polarized collection is parallel to the cylindrical direction of nanopores. As shown in **Figure 4**a and Figure 4c, the polarized PL spectra exhibit a characteristic vibronic progression

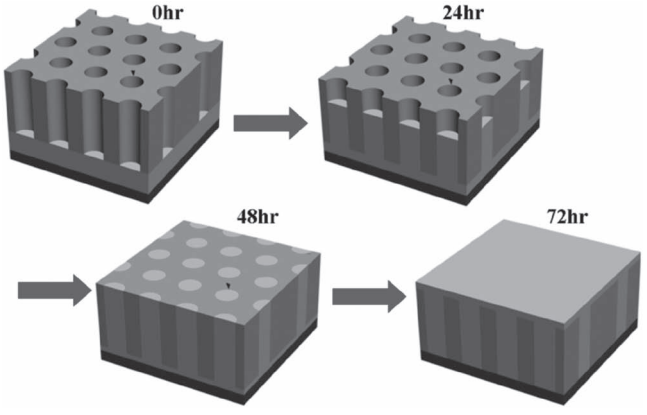

Scheme 1. Schematic illustration of the morphological evolution of pore-filling PVE.

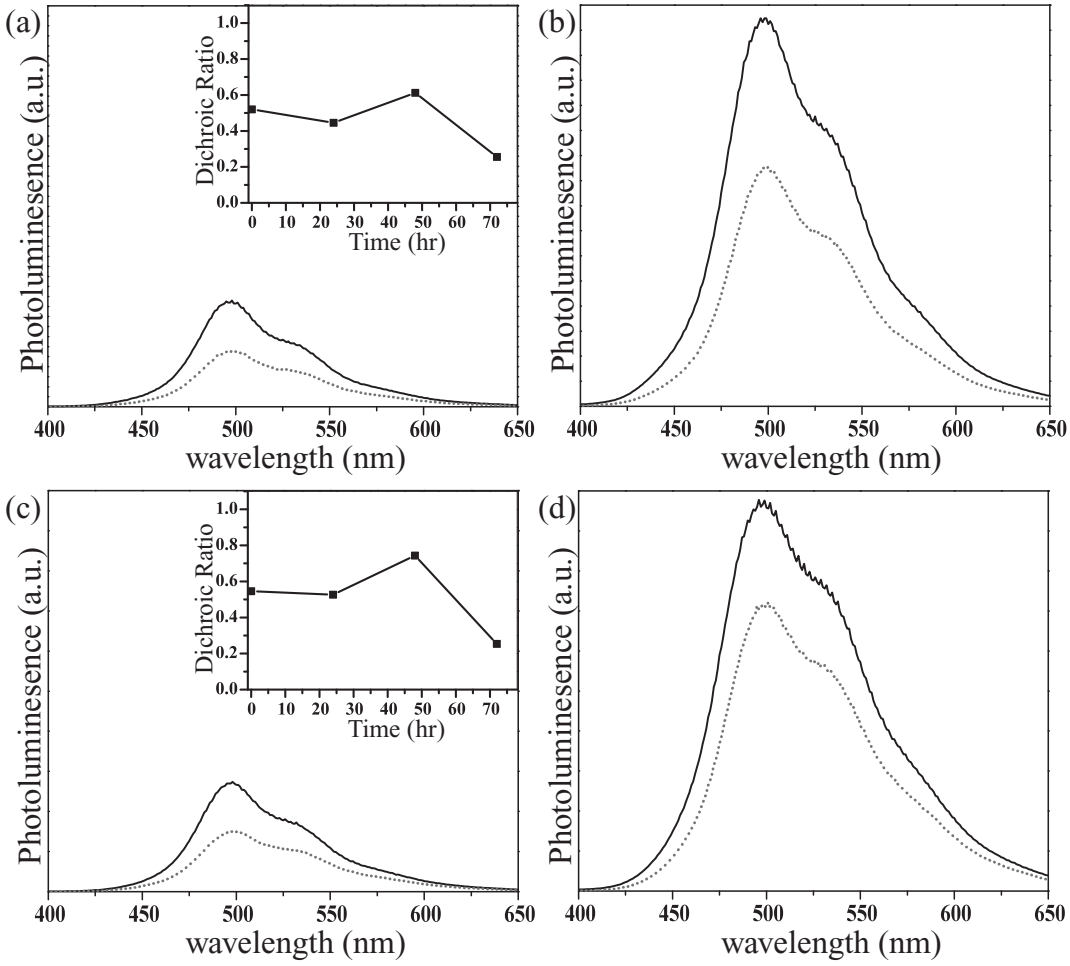

Figure 4. Polarized PL spectra of nanoporous PS templates on spin-coated a,b) PPV3 and c,d) PPV7 thin films for different solvent-annealing times; (a) and (c) corresponding to the annealing time at 0 hr; (b) and (d) corresponding to the annealing time at 48 hr. The spectra were acquired under conditions of vertically polarized excitation with vertically (VV, solid line) or horizontally (VH, dot line) polarized collection. Insets show the plot of DR_E versus annealing time.

with two emission peaks at 498 and 533 nm, assigned to PVE emission. Consistently, the polarized PL intensity of templated PVE nanoarrays significantly increases after solvent annealing for 48 hr (see Figure 4b and Figure 4d). Moreover, DR_E ($DR_E = I_{VH}/I_{VV}$, where I_{VV} and I_{VH} are the PL intensities measured at the 498 nm for each collection polarization) of 0.52 and 0.54 were determined from PVE3 and PVE7 thin films, respectively. The DR_E of PVE7 is slight larger than that of PVE3 before solvent annealing due to molecular weight effect. The plots of in-situ DR_E versus annealing time are also shown in the inset of Figure 4a and Figure 4c. After solvent annealing for 48 hr, the DR_E of templated PVE3 and PVE7 nanoarrays reach a maximum value at 0.61 and 0.74, respectively. In contrast to the DR_E for PVE thin film (i.e., the result before solvent annealing), the DR_E for templated PVE nanoarrays significantly increases. The change is attributed to the reordering of PVE chains within the nanopores during the pore-filling process. Consistently, the DR_E of PVE7 is larger than that of PVE3 after solvent annealing, showing that the templated PVE7 nanoarrays with higher molecular weight (M_w) possesses higher anisotropy of polymer chain parallel to the cylindrical direction of nanopores as compared with the templated PVE3 nanoarrays with lower M_w. These results indicate that the nanoscale spatial effect on the orientation of chain is dependent upon the size of polymer chain; the degree of anisotropy in PVE7 polymer chains with higher M_w should be higher than that in PVE3 polymer with lower M_w. The observed molecular weight effect on the induced alignment is in line with the confinement effect resulting from the consideration of spatial constraint. On the basis of the PL and polarized PL results, we suggest that the chain alignment along the cylindrical direction of nanopores can be induced by nanoscale templating.

To further examine the orientated PVE chains within the nanopores, GI-FTIR measurements were carried out. In GI-FTIR spectroscopy the electrical field vector E is perpendicular to the substrate so that only the functional groups with transition-dipole moment components perpendicular to the substrate can be responsive for the spectroscopic absorption.

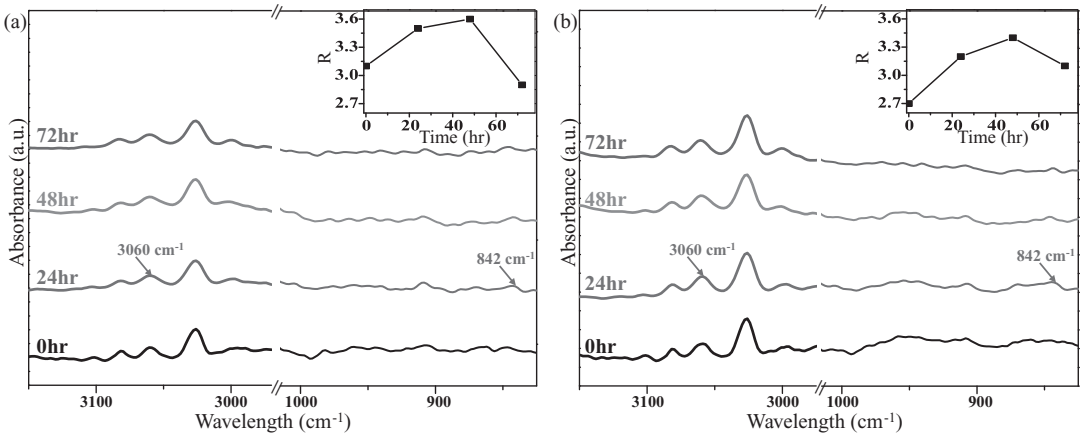

Figure 5. GI-FTIR spectra of nanoporous PS templates on spin-coated a) PPV3 and b) PPV7 thin films for different solvent-annealing times. Insets show the comparison of the $R = A_{3060}/A_{842}$ of the GI-FTIR absorbance at 3060 cm^{-1} and 842 cm^{-1} for different annealing times.

Figure 5a and Figure 5b show in-situ GI-FTIR spectrum of PEV3 and PVE7 within nanoporous PS template for different solvent annealing times. As demonstrated, the differences can be sensitively detected from grazing incidence spectra of PVE thin film and templated PVE nanoarrays. As the transition dipole moment vector of a vibration mode is oriented at a specific angle ϕ relative to the chain axis of PPV backbone, the IR spectra can be used to obtain information on the chain orientation by comparing the relative strength of vibration bands with different ϕ.[44,45] As shown in Figure 5a and Figure 5b, the peak at 842 cm^{-1} is attributed to the vinyl CH out-of-plane deformation with the direction of the transition dipole moment perpendicular to the chains axis ($\phi = 73°$) whereas the peak at 3060 cm^{-1} is referred to the *trans*-vinylene C-H stretch with the direction of the transition dipole moment parallel to the chain axis ($\phi = 30°$), corresponding to the PPV backbone. While the polymer chains are highly oriented to the cylindrical direction, the absorbance of the band at 3060 cm^{-1} ($\phi = 30°$) would be larger. After solvent annealing for 48 hr, the absorbance of band at 3060 cm^{-1} slightly increases, and the absorbance of band at 842 cm^{-1} reduces in the GI-FTIR spectrum, which indicates the backbone segment possessing higher anisotropy parallel to the cylindrical direction of nanopores. The ratio of the absorption bands at 3060 cm^{-1} ($\phi = 30°$) and 842 cm^{-1} ($\phi = 73°$), which is defined as $R = A_{3060}/A_{842}$, was used to quantitatively examine the degree of induced chain alignment. The comparisons of R values are given in the insets of Figure 5a and Figure 5b. The maximum R ratios of 3.6 and 3.3 can be found after solvent annealing for 48 hr in templated PVE3 and PVE7 nanoarrays, respectively. Comparatively, the R ratio of templated PVE nanoarrays is indeed higher than that of PVE thin film, indicating that the degree of chain alignment in templated PVE nanoarrays is indeed higher than that in the intrinsic PVE thin film. The GI-FTIR result for 72 hr is also in line with the observed changes of the polarized PL spectra results, showing that the nanoscale spatial effect is annihilated reintroducing a significant self-quenching problem. Furthermore, time-resolved PL decay experiments were acquired for intrinsic PVE thin film and templated PVE nanoarrays. As shown in **Figure 6**, the PL lifetime of templated PVE nanoarrays is significantly longer than that of PVE thin film. The variation is also in line with the observed changes of PL and polarized PL spectroscopic results. The results of the PL decay experiments reveal that the maximum life time can be found in templated PVE nanoarrays after

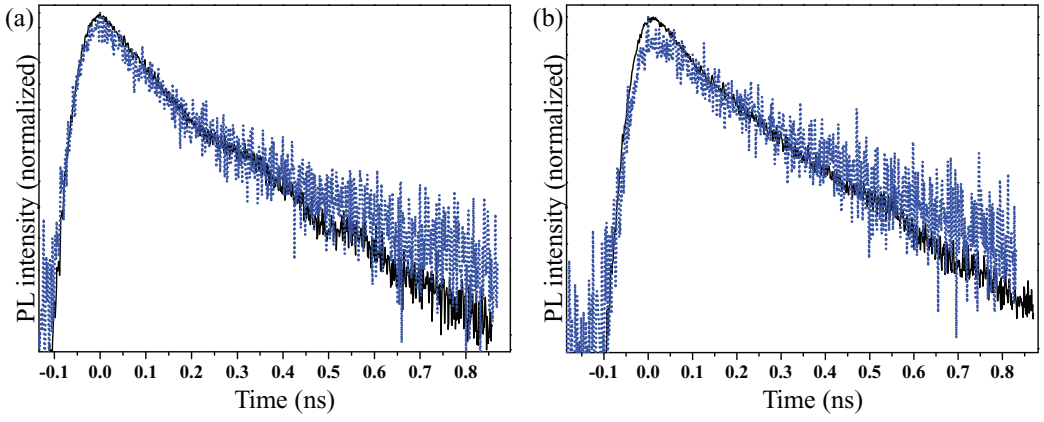

Figure 6. PL decay spectra of nanoporous PS template on spin-coated a) PPV3 and c) PPV7 thin film before (solid line) and after (dot line) solvent annealing time for 48 hr.

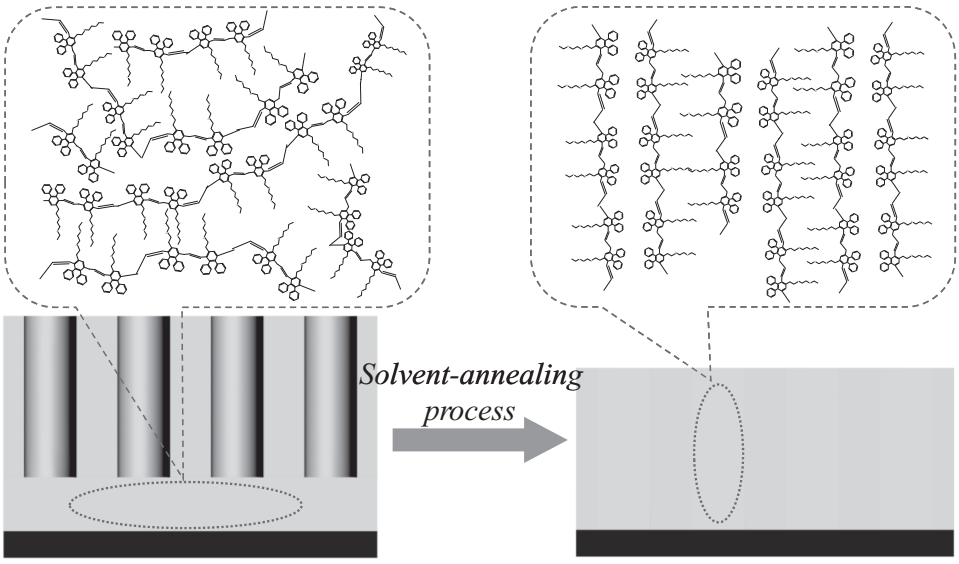

Scheme 2. Illustration of induced chain alignment for spin-coated PVE film at which the formation of oriented polymer chains parallel to the cylindrical direction of nanopores can be achieved by solvent annealing.

solvent annealing for 48 hr and then start to decrease after 72 hr solvent annealing (see SI, Figure S3). In our previous work, the PL results of PPV nanotubes exhibited higher quantum yield and longer lifetime as compared to that of bulk PPV films; suggesting that those improved properties are attributed to the cancellation of interchain interactions.[46]

With the combination of polarized PL and GI-FTIR results, a complete picture of nanoscale spatial effect can be acquired so as to add an isotropic feature for the chain behavior of PVE polymer. As illustrated in **Scheme 2**, PVE polymer chains are successfully pore-filled into the nanochannels from random chain configuration by solvent annealing, and then anisotropic polymer chains parallel to the cylindrical direction of nanopores are induced due to the confinement effect at which the dimension of the polymer chain is approximately half of the diameter of nanoporous PS template (~20 nm). In contrast to intrinsic PVE thin film with random chain configuration, polymer chains in templated PVE nanoarrays possess anisotropic chain orientation parallel to the cylindrical direction of nanopores. Accordingly, a significant enhancement in luminescence can be acquired by pore-filling the PVE into the nanopores due to the nanoscale spatial effect, leading to the observed geometry-dependent chain alignment, which alleviates the self-quenching problem.

3. Conclusions

This work developed a simple method to generate ordered DP-PPV-PEO nanoarrays through a pore-filling process, subsequently enhancing the luminescence. The enhanced luminescence is attributed to the increase of chain alignment in PPV backbone driven by the nanoscale spatial effect for pore-filled PVE. As shown by the SPM observation of morphological evolution and corresponding PL results, the variation on the intensity of PVE emission is correlated with the progress of solvent annealing for pore-filling PVE into nanoporous template. Owing to the enhanced chain alignment of PPV backbone, the self-quenching problem of PVE luminescence can be significantly inhibited. This work also characterized the chain alignment of templated PVE nanoarrays by polarized PL and GI-FTIR experiments, demonstrating the nanoscale spatial effect on the PVE chain orientation with chain alignment parallel to the cylindrical direction of nanopores. Furthermore, the PL decay experiments exhibited that templated PVE nanoarrays indeed give longer fluorescence lifetime. Consequently, the enhanced luminescence of PVE nanostructure driven by the nanoscale spatial effect is highly promising for use in designing luminescent nanodevices.

4. Experimental Section

As shown in Scheme S1, the aldol condensation of Benzil with diethyl-1,3-acetonedicarboxylate using KOH and its derivatives are dehydrated by Ac_2O/H_2SO_4 mixtures to obtain 2,5-dicarbethoxy-3,4-diphenylcyclopentadienone (**1**). Compound **1** undergo Diels–Alder reaction with 5-chloro-1-pentyne to give diethyl 2,3-diphenyl-5-propyl-chloride terephthalate (**2**). In the presence of excess sodium hydride and small amount of potassium iodide, the classic Williamson ether synthesis of **2** and commercially available poly(ethylene oxide) methyl ether with different alkyl-chain lengths (m = 8, 17) in dry THF yielded **3a** and **3b**, respectively. Subsequent reaction of Diethyl 2,3-diphenyl-5-(trimethylene-heptadeca (oxyethylene)-methoxy) terephthalate (**3b**) as example was reduced with $LiAlH_4$ to give 2,3-Diphenyl-5-(trimethylene-heptadeca (oxyethylene)-methoxy)-1,4-bis (hydroxymethyl) benzene (**4b**) which then react with thionyl chloride to give momomer 2,3-diphenyl-5-(trimethylene-heptadeca (oxyethylene)-methoxy)-1,4-bis-(chloromethyl) benznene (**5b**). Finally, the polymerization was carried out via a modified Gilch route with excess amount of *tert*-BuOK in THF to obtain Poly(2,3-diphenyl-5-(trimethylene-heptadeca(oxyethylene)-methoxy)-phenylene vinylene) (DP-PPV-PEO). The details synthesis steps characterization of the polymers and are available in Supporting Information.

The general pore-filling methods were as follows: PS-PLLA diblock copolymers with a PLLA volume fraction of 0.25 were prepared by two-step living polymerization in sequence.[37,38] A thin-film sample with

perpendicular cylindrical nanostructures was initially formed onto a glass substrate by spin-coating (1000 rpm) from a 1.0 wt% dilute solution of PS-PLLA at 50 °C; the film thickness was about 60 nm. After dried in a vacuum overnight, the film was exposed to UV radiation (wavelength at 254 nm) under a vacuum for over 10 min. The thin-film sample was then placed in NaOH solution for 4 days to degrade PLLA and, finally, dispersed in the MeOH solution to wash out residual degradation solution. After hydrolysis, the nanoporous PS template was used for pore-filling of PVE polymer. The PVE polymer was synthesized as above. As illustrated in Scheme S2, a specific solvent-annealing process was designed to increase the pore-filling efficiency. The template was removed from a glass substrate with 1% HF solution and, then, floated onto an aqueous surface, finally collected by a glass substrate coated with the PVE thin film (Scheme S2c). The PVE thin film was spin coated 1000 rpm with 2 wt% acetic acid solution (ca. 120 nm in thickness). While PVE film was placed under the nanoporous template (Scheme S2d) and then annealed at acetic acid vapor for different time periods, the PVE was introduced into the pores driven by the capillary force (Scheme S2e). By considering the accuracy for the examination of nanoscale spatial effect, the same samples were used for the GI-FTIR, PL and polarized PL and time-resolved PL experiments. For the precisely comparison, the results were originated from a series of measurements of the same nanoporous PS templates on spin-coated PPV thin film for different annealing times.

Supporting Information

Supporting Information is available from the Wiley Online Library or from the author.

Acknowledgements

The authors would like to thank the National Science Council of the Republic of China, Taiwan, for financially supporting this research under Contract No. NSC 98-2218-E-009-009-MY3 and NSC 99-2120-M-007-003. Also, the authors thank Dr. Jean-Yves Mevellec at CNRS for his help with GI-FTIR experiments.

Received: December 7, 2010
Revised: February 23, 2011
Published online: May 30, 2011

[1] D. Gebeyehu, C. J. Brabec, F. Padinger, T. Fromherz, J. C. Hummelen, D. Badt, H. Schindler, N. S. Sariciftci, *Synth. Met.* **2001**, *118*, 1.
[2] H. Hoppe, N. S. Sariciftci, *J. Mater. Res.* **2004**, *19*, 1924.
[3] R. H. Friend, R. W. Gymer, A. B. Holmes, J. H. Burroughes, R. N. Marks, C. Taliani, D. D. C. Bradley, D. A. Dos Santos, J. L. Bredas, M. Lögdlund, W. R. Salaneck, *Nature* **1999**, *397*, 121.
[4] B. S. Ong, Y. L. Wu, P. Liu, S. Gardner, *J. Am. Chem. Soc.* **2004**, *126*, 3378.
[5] T. L. Benanti, D. Venkataraman, *Photosynth. Res.* **2006**, *87*, 73.
[6] A. L. Briseno, S. C. B. Mannsfeld, S. A. Jenekhe, Z. Bao, Y. Xia, *Mater. Today* **2008**, *11*, 38.
[7] G. Gustafsson, O. Inganas, S. Stafstrom, *Solid State Commun.* **1990**, *76*, 203.
[8] J. H. Burroughes, D. D. C. Bradley, A. R. Brown, R. N. Marks, K. MacKay, R. H. Friend, P. L. Burn, A. B. Holmes, *Nature (London)* **1990**, *347*, 539.
[9] G. Gustafsson, Y. Gao, G. M. Treacy, F. Klavener, N. Colinari, A. J. Heeger *Nature* **1992**, *357*, 477.
[10] A. R. Brown, D. D. C. Bradley, J. H. Burroughes, R. H. Friend, N. C. Greemham, P. L. Burn, A. B. Holmes, A. Kraft, *Appl. Phys. Lett.* **1992**, *61*, 2793.
[11] A. R. Brown, N. C. Greemham, J. H. Burroughes, D. D. C. Bradley, R. H. Friend, P. L. Burn, A. Kraft, *Chem. Phys. Lett.* **1992**, *200*, 46.
[12] G. Duda, A. J. Schouten, T. A. Arndt, G. Lieser, G. F. Schmidt, C. Bubeck, G. Wegner, *Thin Solid Films* **1988**, *159*, 221.
[13] R. H. G. Brinkhuis, A. J. Schouten, *Macromolecules* **1992**, *25*, 2717.
[14] T. Sauer, T. Arndt, D. Batchelder, A. A. Kalachev, G. Wegner, *Thin Solid Films* **1990**, *187*, 357.
[15] M. Jandke, P. Strohriegl, J. Gmeiner, W. Brütting, M. Schwoerer, *Adv. Mater.* **1999**, *11*, 1518.
[16] M. Aryal, K. Trivedi, W. C. Hu, *ACS Nano* **2009**, *3*, 3085.
[17] B. Frank, A. P. Gast, T. P. Russell, H. R. Brown, C. J. Hawker, *Macromolecules* **1996**, *29*, 6531.
[18] X. Zheng, B. B. Sauer, J. G. Van Alsten, S. A. Schwarz, M. H. Rafailovich, J. Sokolov, M. Rubinstein, *Phys. Rev. Lett.* **1995**, *74*, 407.
[19] R. L. Jones, S. K. Kumar, D. L. Ho, R. M. Briber, T. P. Russell, *Nature,* **1999**, *400*, 146.
[20] K. Shin, S. Obukhov, J. T. Chen, J. Huh, Y. Hwang, S. Mok, P. Dobriyal, P. Thiyagarajan, T. P. Russell, *Nature Mater.* **2007**, *6*, 961.
[21] H. R. Brown, *Science* **1994**, *263*, 1411.
[22] K. Y. Suh, H. H. Lee, *Adv. Mater.* **2001**, *13*, 1386.
[23] K. Shin, H. Q. Xiang, S. I. Moon, T. Kim, T. J. McCarthy, T. P. Russell. *Science* **2004**, *306*, 76.
[24] M. Steinhart, R. B. Wehrspohn, U. Gösele, J. H. Wendorff, *Angew. Chem.Int. Ed.* **2004**, *43*, 1334.
[25] D. O'Carroll, D. Iacopino, A. O'Riordan, P. Lovera, E. O'Connor, G. A. O'Brien, G. Redmond, *Adv. Mater.* **2008**, *20*, 42.
[26] F. S. Bates, G. H. Fredrickson, *Annu. Rev. Phys. Chem.* **1990**, *41*, 525.
[27] T. L. Morkved, M. Lu, A. M. Urbas, E. E. Ehrichs, H. M. Jaeger, P. Mansky, T. P. Russell, *Science* **1996**, *273*, 931.
[28] P. Mansky, Y. Liu, E. Huang, T. P. Russell, C. Hawker, *Science* **1997**, *275*, 1458.
[29] J. Y. Cheng, C. A. Ross, V. Z.-H. Chan, E. L. Thomas, R. G. H. Lammertink, G. J. Vancso, *Adv. Mater.* **2001**, *13*, 1174.
[30] K. Temple, K. Kulbaba, K. N. Power-Billard, I. Manners, K. A. Leach, T. Xu, T. P. Russell, C. J. Hawker, *Adv. Mater.* **2003**, *15*, 297.
[31] S. H. Kim, M. J. Misner, T. Xu, M. Kimura, T. P. Russell, *Adv. Mater.* **2004**, *16*, 226.
[32] T. Thurn-Albrecht, R. Steiner, J. DeRouchey, C. M. Stafford, E. Huang, M. Bal, M. Tuominen, C. J. Hawker, T. P. Russell, *Adv. Mater.* **2000**, *12*, 787.
[33] M. J. Misner, H. Skaff, T. Emrick, T. P. Russell, *Adv. Mater.* **2003**, *15*, 221.
[34] J. Y. Cheng, C. A. Ross, E. L. Thomas, H. I. Smith, G. J. Vancso, *Appl. Phys. Lett.* **2002**, *81*, 3657.
[35] R. M. Ho, W. H. Tseng, H. W. Fan, Y. W. Chiang, C. C. Lin, B. T. Ko, B. H. Huang, *Polymer* **2005**, *46*, 9362.
[36] A. S. Zalusky, R. Olayo-Valles, C. J. Taylor, M. A. Hillmyer, *J. Am. Chem. Soc.* **2001**, *123*, 1519.
[37] B. T. Ko, C. C. Lin, *J. Am. Chem. Soc.* **2001**, *123*, 7973.
[38] R. M. Ho, Y. W. Chiang, C. C. Tsai, C. C. Lin, B. T. Ko, B. H. Huang, *J. Am. Chem. Soc.* **2004**, *126*, 2704.
[39] Y. T. Tseng, W. H. Tseng, C. H. Lin, R. M. Ho, *Adv. Mater.* **2007**, *19*, 3584.
[40] K. H. Lo, W. H. Tseng, R. M. Ho, *Macromolecules* **2007**, *40*, 2621.
[41] K. H. Lo, M. C. Chen, R. M. Ho, H. W. Sung, *ACS Nano* **2009**, *3*, 2660.
[42] S. J. Chung, J. I. Jin, C. H. Lee, C. E. Lee, *Adv. Mater.* **1998**, *9*, 684.
[43] T. C. Wang, H. Y. Hsueh, R. M. Ho, *Chem. Mater.* **2010**, *22*, 4642.
[44] N. B. Colthup, L. H. Daly, S. E. Wiberley, *Introduction to Infrared and Raman Spectroscopy*; Academic Press, New York, **1964**.
[45] D. D. C. Bradley, R. H. Friend, H. Lindenberger, S. Roth, *Polymer* **1986**, *27*, 1709.
[46] F. Massuyeau, J. L. Duvail, H. Athalin, J. M. Lorcy, S. Lefrant, J. W´ery, E. Faulques, *Nanotechnology* **2009**, *20*, 155701.